Notes

Contribution from the School of Chemical Sciences, University of Illinois at Urbana-Champaign, Urbana, Illinois 61801, and Department of Chemistry, University of Oregon, Eugene, Oregon 97403

Characterization of Very Large Polyoxoanions by Fast Atom Bombardment Mass Spectroscopy (FABMS)

Kenneth S. Suslick,*† J. Carter Cook,† Brian Rapko,‡ Michael W. Droege,‡ and Richard G. Finke*‡

Received May 21, 1985

The development of the chemistry of polyoxoanions has been frustrated by well-known difficulties in obtaining full characterization of such compounds.[1] The potential importance of these complexes in a variety of applications (including their use as catalysts,[2] as photocatalysts,[3] as soluble metal oxide analogues,[4] and as electron microscopy labels[5]) recently led us to utilize fast atom bombardment mass spectroscopy (FABMS)[6,7] to obtain the first mass spectra of smaller polyoxoanions.[8] Herein we report the first FABMS of very large, highly charged, nonvolatile polyoxoanion salts with molecular weights of 4000–8000 daltons. In addition, we have demonstrated the utility of FABMS in establishing the molecular formulas of new, uncharacterized polyoxoanions: e.g., the previously unknown $(Bu_4N)_7HSi_2W_{18}Zr_3O_{68}\cdot xH_2O$ (Bu_4N^+ = tetra-*n*-butylammonium cation).

Experimental Section

All FABMS spectra were obtained on a VG Analytical, Ltd., ZAB-HF ultrahigh-resolution double-focusing mass spectrometer equipped with an 11/250 data system. Milligram samples were dissolved in ~100 μL of CH_3CN, and 1 μL of this solution was then added to ~2 μL of 5:1 dithiothreitol/dithioerythritol directly placed on the target. Other low-volatility matrices that have worked with FABMS of polyoxoanions include thioglycerol, triethylenetetramine, and dimethylformamide. Ions (at accelerating potentials of 3–4 kV) were generated from impact on the target matrix of a neutral Xe atom beam (derived from a Xe^+ ion beam at an accelerating potential of 8 kV); typical ion currents were $\sim 10^{-13}$ A. All spectra were analyzed by comparison to isotopic molecular ion distributions calculated via the ISO program of VG Analytical.

The synthesis of $(Bu_4N)_6[H_2Si_2W_{18}Nb_6O_{77}]$ has been reported in detail elsewhere.[4b] Briefly, $K_7HNb_6O_{19}\cdot 13H_2O$ is dissolved in H_2O_2, acidified with HCl, and then A-β-$Na_9HSiW_9O_{34}\cdot 23H_2O$ is added. All peroxides are removed by treatment with $NaHSO_3$. The resulting anion is precipitated by addition of Bu_4NBr and recrystallization is accomplished from CH_3CN/aqueous HCl. This species has been fully characterized by elemental analysis, IR, solution molecular weight, and ^{183}W NMR data. The previously uncharacterized $(Bu_4N)_7HSi_2W_{18}O_{68}(Zr(OH_2)_x)_3$, where x = 1 or 2, was prepared[4c] by the addition of A-β-$Na_9HSiW_9O_{34}\cdot 23H_2O$ to a strongly acidic aqueous solution of $Zr(O)(SO_4)\cdot H_2SO_4\cdot 3H_2O$ (purchased from Alfa-Ventron Chemicals), followed by precipitation with Bu_4NBr and recrystallization from CH_3CN/CH_2Cl_2.

Results and Discussion

Figure 1A shows the low-resolution (1:1000) negative ion spectrum of $(Bu_4N)_6[H_2Si_2W_{18}Nb_6O_{77}]$.[4b] High m/z peaks correspond to a simple cation-exchange process involving $[(Bu_4N)_{6-n}H_{1+n}Si_2W_{18}Nb_6O_{77}]^-$, where n = 0–6, with increasing loss of oxygen atoms at lower masses, as clearly shown in these peaks' fine structures. At m/z <5000, peaks due to sequential loss of WO_3 fragments (m/z 232) are seen, which is characteristic of polyoxotungstates.[8] Figure 1B shows the corresponding low-resolution positive ion spectrum. The parent ion peak, C, at m/z 6613 due to $[(Bu_4N)_6H_3Si_2W_{18}Nb_6O_{77}]^+$ is quite pronounced, with other peaks due to cation exchange. Much less tendency toward

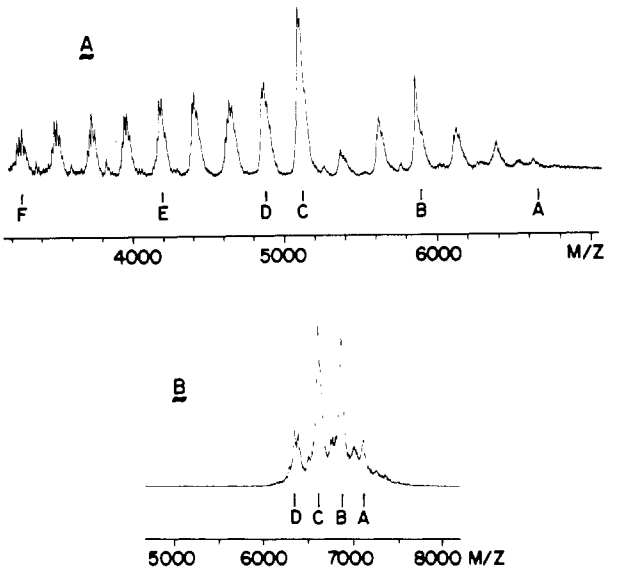

Figure 1. Part A: Negative ion FABMS of $(Bu_4N)_6[H_2Si_2W_{18}Nb_6O_{77}]$ (where M = $Si_2W_{18}Nb_6O_{77}$): A, $[M + [H] + 6[Bu_4N]]^-$; B, $[M + 4[H] + 3[Bu_4N] - 2[O]]^-$; C, $[M + 7[H] - 4[O]]^-$; D, $[M + 7[H] - 4[O] - [WO_3]]^-$; E, $[M + 7[H] - 4[O] - 4[WO_3]]^-$; F, $[M + 7[H] - 4[O] - 8[WO_3]]^-$. Part B: Positive ion FABMS of $(Bu_4N)_6[H_2Si_2W_{18}Nb_6O_{77}]$ (where M = $Si_2W_{18}Nb_6O_{77}$): A, $[M + [H] + 8[Bu_4N]]^+$; B, $[M + 2[H] + 7[Bu_4N]]^+$; C, $[M + 3[H] + 6[Bu_4N]]^+$; D, $[M + 4[H] + 5[Bu_4N] - [O]]^+$.

(1) (a) Pope, M. T. "Heteropoly and Isopoly Oxometalates"; Springer-Verlag: New York, 1983; Inorganic Chemistry Concepts 8. Evans, H. T., Jr.; Pope, M. T. *Inorg. Chem.* **1984**, *23*, 501. (b) Finke, R. G.; Droege, M. W. *Inorg. Chem.* **1983**, *22*, 1006.
(2) (a) Kozhevnikov, I. V.; Matveev, K. I. *Appl. Catal.* **1983**, *5*, 135. (b) Kozhevnikov, I. V.; Matveev, K. I. *Russ. Chem. Rev. (Engl. Transl.)* **1982**, *51*, 1075. (c) Baba, T.; Sakai, J.; Ono, Y. *Bull. Chem. Soc. Jpn.* **1982**, *55*, 2657.
(3) (a) Papaconstantinou, E. *J. Chem. Soc., Chem. Commun.* **1982**, 12. (b) Yamase, T. *Inorg. Chim. Acta* **1983**, *76*, L25. (c) Yamase, T. *Inorg. Chim. Acta* **1981**, *54*, L207. (d) Yamase, T.; Sasaki, R.; Ikawa, T. *J. Chem. Soc., Dalton Trans.* **1981**, 628.
(4) (a) Finke, R. G.; Droege, M.; Hutchinson, J. R.; Gansow, O. *J. Am. Chem. Soc.* **1981**, *103*, 1587. (b) Finke, R. G.; Droege, M. W. *J. Am. Chem. Soc.* **1984**, *106*, 7274. (c) Finke, R. G.; Rapko, B., manuscript in preparation. (d) Finke, R. G.; Rapko, B. *Organometallics*, in press. (e) Finke, R. G.; Rapko, B.; Saxton, R. J.; Domaille, P. J. *J. Am. Chem. Soc.*, in press. (f) Day, V. W.; Klemperer, W. G. *Science (Washington, D.C.)* **1985**, *228*, 533 and references therein.
(5) (a) Zonnevijlle, F.; Pope, M. T. *J. Am. Chem. Soc.* **1979**, *101*, 2731. (b) Mann, S.; Williams, R. J. P.; Sethuraman, P. R.; Pope, M. T. *J. Chem. Soc., Chem. Commun.* **1981**, 1083. (c) Keana, J. F. W.; Ogan, M. C.; Lü, Y.; Beer, M.; Varkey, J. *J. Am. Chem. Soc.* **1985**, *107*, 6714.
(6) (a) Rinehart, K. L., Jr. *Science (Washington, D.C.)* **1982**, *218*, 254. Busch, K. L.; Cooks, R. G. *Science (Washington, D.C.)* **1982**, *218*, 247. (b) Barber, M.; Bordoli, R. S.; Elliot, G. J.; Sedgwick, R. D.; Tyler, A. N. *Anal. Chem.* **1982**, *54*, 645A. (c) Devienne, F. M.; Roustan, J.-C. *Org. Mass. Spectrom.* **1982**, *17*, 173. (d) Franks, J. *Int. J. Mass Spectrom. Ion. Phys.* **1983**, *46*, 343. (e) Martin, S. A.; Costello, C. E.; Biemann, K. *Anal. Chem* **1982**, *54*, 2362. (f) Caprioli, R. M. *Anal. Chem.* **1983**, *55*, 2387.
(7) (a) Davis, R.; Groves, I. F.; Durrant, J. L. A.; Brooks, P.; Lewis, I. *J. Organomet. Chem.* **1983**, *241*, C27. (b) Miller, J. M. *J. Organomet. Chem.* **1983**, *249*, 299; *Adv. Inorg. Chem. Radiochem.* **1984**, *28*, 1. (c) Cerny, R. L.; Sullivan, B. P.; Bursey, M. M.; Meyer, T. J. *Anal. Chem.* **1983**, *55*, 1954. (d) Cerny, R. L.; Sullivan, B. P.; Bursey, M. M.; Meyer, T. J. *Inorg. Chem.* **1985**, *24*, 397. (e) Cerny, R. L.; Bursey, M. M.; Jameson, D. L.; Malachowski, M. R.; Sorrell, T. N. *Inorg. Chim. Acta* **1984**, *89*, 89. (f) Lumenthal, T. B.; Bruce, M. I.; Shawkataly, O. B.; Green, B. N.; Lewis, I. *J. Organomet. Chem.* **1984**, *269*, C10. (g) Freas, R. B.; Campana, J. E. *Inorg. Chem.* **1984**, *23*, 4654.

†University of Illinois at Urbana-Champaign.
‡University of Oregon.

0020-1669/86/1325-0241$01.50/0

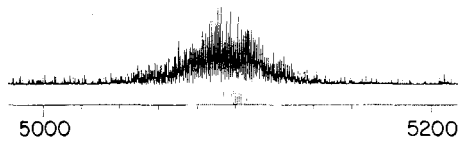

Figure 2. High-resolution (1:6000) negative ion FABMS of $(Bu_4N)_6[H_2Si_2W_{18}Nb_6O_{77}]$. The observed spectrum corresponds to peak C of Figure 1A. The inset represents the calculated isotopic distribution of just $[H_7Si_2W_{18}Nb_6O_{73}]^-$.

fragmentation is observed in the positive ion FABMS, which aids in compound identification.

There are inherent limitations in the utility of *high*-resolution mass spectra with very high molecular weight ions. Unlike mass spectra of low molecular weight compounds, high m/z ions do not necessarily correspond to a single, well-defined atomic composition.[9] For example, at unit resolution, multiple isotopic combinations can yield the same mass. Furthermore, the isotopic distribution of the high molecular weight ions is inherently broad due to the isotopic multiplicity of the component elements (e.g. ^{180}W had 0.14% natural abundance, ^{182}W has 26.41%, ^{183}W has 14.4%, ^{184}W has 30.6%, and ^{186}W has 28.41%). In our cases, the calculated range ($\Delta m/z$) of isotopic composition for which peaks are $\geq$10% of the most probable m/z is $\sim$30; the situation is only slightly improved in large organic polymers.[9] In order to accurately interpret the observed high-resolution spectra, one must make a complete simulation of all isotopic combinations. The calculated most abundant mass ion will *not* be the same as the monoisotopic mass ion[9] (calculated from the most abundant isotope of each element) and will *not* be the same as the average mass calculated from each element's average atomic weight. For example, $[H_7Si_2W_{18}Nb_6O_{73}]^-$ has a calculated most abundant mass of 5097, but the monoisotopic mass is 5099.2, and the average atomic weights give a mass of 5097.9. Only the first of these is relevant to the observed mass spectrum. This discrepancy can be much worse for organic polymers (where all minor isotopes are of higher atomic weight than the most abundant).[9]

With these caveats in mind, we have also obtained the high-resolution (1:6000) mass spectrum of these polyoxoanions. Figure 2 shows a portion of such a FABMS for $(Bu_4N)_6[H_2Si_2W_{18}Nb_6O_{77}]$, which corresponds to peak C in Figure 1A, together with the simulation of the isotopic distribution expected for $[H_7Si_2W_{18}Nb_6O_{73}]^-$. The observed spectrum has overlapping contributions (due to progressive O atom loss) from $[H_7Si_2W_{18}Nb_6O_x]^-$ where x = 77–71. This progression is perhaps most clearly seen in the fine structure of the lower resolution spectra and is a feature common to FABMS of polyoxoanions.[8]

We have extended our use of FABMS to establish the molecular formula of new, previously uncharacterized polyoxoanions. For example, the FABMS of a pure compound that elemental analysis gives as $[(Bu_{3.5}N)_4SiW_9Zr_{1.5}O_x]_n$[4c] ($x$ = 35 ± 2 by oxygen analysis) is shown in Figure 3. The low-resolution (1:1500) negative ion spectrum, Figure 3A, shows peaks assignable to $[(Bu_4N)_{6-n}H_{1+n}Si_2W_{18}Zr_3O_{68}]^-$ for n = 0–6 (with increasing O loss at lower mass) and small but real peaks in between due to ZrO_2 (m/z 123) loss. The positive ion spectrum, Figure 3B, is again especially informative and shows a series of peaks assignable to $[(Bu_4N)_{8-n}H_{1+n}Si_2W_{18}Zr_3O_{68}]^+$ where n = 0–3 as well as intervening ZrO_2 loss peaks. *From elemental analysis and FABMS alone*, a molecular formula of $(Bu_4N)_7HSi_2W_{18}Zr_3O_{68}$ results with reasonable confidence. On the basis of the known structures[10a,b] of $P_2W_{18}(WO)_3O_{68}^{6-}$, $P_2W_{18}(CoOH_2)_3O_{68}^{12-}$, and related compounds,[10c] we conclude that the final molecular formula is $(Bu_4N)_7HSi_2W_{18}O_{68}(Zr(OH_2)_x)_3$, where x = 1 or 2; additional studies are in progress.[4c]

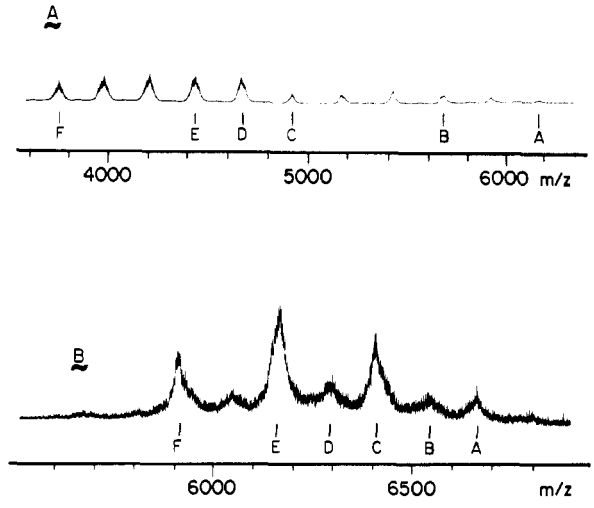

Figure 3. Part A: Negative ion FABMS of $(Bu_4N)_7HSi_2W_{18}Zr_3O_{68}\cdot xH_2O$ (where M = $Si_2W_{18}Zr_3O_{68}$): A, $[M + [H] + 6[Bu_4N]]^-$; B, $[M + 3[H] + 4[Bu_4N] - [O]]^-$; C, $[M + 6[H] + [Bu_4N] - 3[O]]^-$; D, $[M + 7[H] - 3[O]]^-$; E, $[M + 7[H] - 3[O] - [WO_3]]^-$; F, $[M + 7[H] - 3[O] - 4[WO_3]]^-$. Part B: Positive ion FABMS of $(Bu_4N)_7HSi_2W_{18}Zr_3O_{68}\cdot xH_2O$ (where M = $Si_2W_{18}Zr_3O_{68}$): A, $[M + [H] + 8[Bu_4N]]^+$; B, $[M + [H] + 8[Bu_4N] - [ZrO_2]]^+$; C, $[M + 2[H] + 7[Bu_4N] - [O]]^+$; D, $[M + 2[H] + 7[Bu_4N] - [O] - [ZrO_2]]^+$; E, $[M + 3[H] + 6[Bu_4N] - [O]]^+$; F, $[M + 4[H] + 5[Bu_4N] - [O]]^+$.

Present evidence on the mechanisms of ion formation during FAB suggests that the observed ions are due to a cascade of ionization and subsequent hydrogen radical abstraction from the matrix.[11] Thus, the negative ions are generated by the attachment of solvated electrons to the polyoxo cluster, followed by solvent H atom abstraction and immediate loss of O, H_2O, or WO_3 (i.e., redox fragmentation),[7c,d] due to the weakened bonding within the reduced and protonated cluster. Positive ion FABMS would be expected, therefore, to show less fragmentation than negative ion FABMS, as observed. Such an ionization scheme also explains why we have observed[8] $H_5SiW_{12}O_{40}^+$ as a major peak in the positive ion FABMS of $H_4SiW_{12}O_{40}$ in dithiothreitol/dithioerythritol solutions, even though this latter compound is a strong acid in aqueous solution.[8] Initial ionization (eq 1), followed by H· abstraction from the solvent, RSH (eq 2), readily explains the

$$H_4SiW_{12}O_{40} + Ar(fast) \rightarrow H_4SiW_{12}O_{40}^+\cdot + e^- + Ar \quad (1)$$

$$H_4SiW_{12}O_{40}^+\cdot + RSH \rightarrow H_5SiW_{12}O_{40}^+ + RS\cdot \quad (2)$$

otherwise puzzling, strong peak due to $H_5SiW_{12}O_{40}^+$. These considerations suggest that FABMS will be of limited use in cases where the compound is not stable to the initial ionization process[12] or suffers matrix damage from reaction with the H^+ and/or e^- produced.

Certain supported organometallics, such as $(OC)_3Re\cdot SiW_9N_3O_{40}^{6-}$, show net loss of the organometallic (i.e., only the $SiW_9V_3O_{40}^{7-}$ fragment is observed) in the FABMS. Initial ionization at the metal of the organometallic (Re) and secondary reactions with the matrix are one plausible explanation for this observation. Consistent with this, organometallics with a non-ionizable, d^0 metal such as $CpTi\cdot SiW_9V_3O_{40}^{4-}$, exhibit a clean and useful FABMS.[8] Alternatively, reduction of the organometallic by solvated e^- and/or H^+ addition to the polyoxoanion, thus weakening of the organometallic–polyoxoanion bonding, may be involved.

In summary, FABMS constitutes a new and important tool for the rapid characterization of massive polyoxoanions and, by inference, other inorganic polyanions and -cations. Mass spectra

(8) Finke, R. G.; Droege, M. W.; Cook, J. C.; Suslick, K. S. *J. Am. Chem. Soc.* **1984**, *106*, 5750.
(9) (a) Yergey, J.; Heller, D.; Hansen, G.; Cotter, R. J.; Fenselau, C. *Anal. Chem.* **1983**, *55*, 353. (b) Busch, K. L.; Glish, G. L. *BioTechniques* **1984**, *2* (May/June), 128.
(10) (a) Pope, M. T. "Heteropoly and Isopoly Oxometalates"; Springer-Verlag: New York, 1983; Inorganic Chemistry Concepts 8, p 68. (b) Knoth, W. H.; Domaille, P. J.; Farlee, R. D. *Organometallics* **1985**, *4*, 62. (c) Robert, F.; Leyrie, M.; Herve, G. *Acta Crystallogr., Sect. B: Struct. Crystallogr. Cryst. Chem.* **1982**, *B38*, 358.
(11) Clayton, E.; Wakefield, A. J. C. *J. Chem. Soc., Chem. Commun.* **1984**, 969.

of inorganic complexes with molecular weights as high as 20000 amu undoubtedly will be obtained by this technique in the near future.

Acknowledgment. Support at Oregon by NSF Grant CHE-8313459 to R.G.F. and at Illinois by NSF Grant CHE-8020006 to K.S.S. is gratefully acknowledged. R.G.F. has been supported as a Dreyfus Teacher-Scholar (1982-1987) and an Alfred P. Sloan Fellow (1982-1984); K.S.S. is an Alfred P. Sloan Fellow (1985-1987) and recipient of an NIH Research Career Development Award (1985-1990). FAB mass spectra were obtained in the mass spectroscopy facility of the School of Chemical Sciences, University of Illinois, supported in part by NIH Grant GM-27029; the ZAB mass spectrometer was purchased in part by grants from the NIH Division of Research Resources (RR01575) and from the NSF (PCM-8121494).

Registry No. $(Bu_4N)_6[H_2Si_2W_{18}Nb_6O_{77}]$, 92844-06-9; $(Bu_4N)_7HSi_2W_{18}O_{68}(ZrOH_2)_3$, 99593-28-9; $(Bu_4N)_7HSi_2W_{18}O_{68}(Zr(OH_2)_2)_3$, 99593-27-8.

Contribution from the Departments of Chemistry, University of York, Heslington, York YO1 5DD, U. K., and University of California, Riverside, California 92521

Kinetics of the Reaction of Palladium(II) with Various Dienes and the Importance of the Diene Conformation

Jamil K. K. Sarhan,† Siew-Wan Foong Murray,† Hasan M. Asfour,† Michael Green,*† Richard M. Wing,‡ and Miguel Parra-Haake‡

Received March 27, 1985

The reactions of dienes with palladium(II) to give chelated diene complexes are of interest in three areas: first, the extent to which the conformation of the diene has to be changed after reaction of the first double bond before coordination of the second can occur, i.e. after reaction 1 and before reaction 2; second, whether

$$PdCl_3(OCMe_2)^- + \text{diene} \rightleftharpoons Pd(\eta^2\text{-diene})Cl_3^- + Me_2CO \quad (1)$$

$$Pd(\eta^2\text{-diene})Cl_3^- \rightleftharpoons Pd(\eta^4\text{-diene})Cl_2 + Cl^- \quad (2)$$

the most favorable conformation the diene can adopt is particularly good for formation of $Pd(diene)Cl_2$ and vice versa; third, in obtaining quantitative data relevant to the Wacker process since in these reactions palladium is formed (as a result of hydroxypalladation) much less readily than in the corresponding monoene systems.

The reactions of $Na[PdCl_3(OCMe_2)]$[1] with 1,5-cyclooctadiene (1,5-COD), 1,5-cyclononadiene (1,5-CND), norbornadiene (NBD) and 1,5-hexadiene (1,5-HD) have been studied in 2% aqueous acetone (viz. 1:49 (v:v) water:acetone) by using changes in ultraviolet and ^1H NMR spectra. The processes follow reactions 1 and 2; complexes are formed in which the diene is bonded through one and then two C=C links. On the basis of the kinetic and equilibrium studies below, the speeds and completeness of the reactions of the four dienes can be summarized qualitatively as in Table I.

Kinetics

The positions of the CH=CH resonances in the $Pd(diene)Cl_2$ complexes and the parent dienes are quite distinct; see Table II. In solutions ca. 10^{-2} M in $PdCl_3(OCMe_2)^-$ and in the diene at ca. 25 °C, these $Pd(diene)Cl_2$ peaks become apparent on the order of minutes for NBD and 1,5-COD and of hours for 1,5-CND and 1,5-HD, suggesting very approximate rate constants of 0.05, 1, 10^{-4}, and 10^{-4} M^{-1} s^{-1}. No free diene can be detected at the end of the reactions of NBD and 1,5-COD, but in the case of 1,5-CND and 1,5-HD, completion is not reached even after some 2 days. After a few minutes of reaction by 1,5-CND and 1,5-HD, CH=CH peaks different from those of either free diene or $Pd(diene)Cl_2$ are formed, which we attribute to $Pd(diene)Cl_3^-$, see Table II.

Changes in absorbance at 380-410 nm between 15 and 30 °C on solutions ca. 4×10^{-4} M in $PdCl_3(OH_2)^-$ and 3.3×10^{-2} to 1.6×10^{-1} M in diene over time spans of 15 s to 24 h reveal the following. 1,5-CND and 1,5-HD show an initial fast reaction that fits eq 3,[6,7] followed by a slow step with a rate independent of diene

$$k_{obsd} = k_a[\text{diene}] + k_b \quad (3)$$

concentration and with a rate constant at 25.0 °C approximately equal to those determined by NMR data. Thus the UV and NMR data are fully compatible with the occurrence of (reversible) reactions 1 and 2 ($k_a \equiv k_1$ and $k_b \equiv k_{-1}$). For 1,5-CND and 1,5-HD, equilibrium studies were also made to study reaction 1, aliquots of diene being added to the palladium ion. The customary Hill plots of $(A_0 - A_x)/(A_\infty - A_0)$ against [diene][8] were linear, thus also demonstrating that free Cl^- is not produced during reaction 1 and also giving values of K_1; see Table III.

Analogous experiments on NBD show only one fast step, obeying eq 4. The failure to detect $Pd(diene)Cl_3^-$ with NMR

$$k_{obsd} = k_a[\text{diene}] \quad (4)$$

suggests that (2) is now fast compared with (1). Thus k_a corresponds to K_1k_2 (see Table III), while the absence of a k_b term indicates that (2) proceeds to "completion".

In the case of 1,5-COD, graphs of $\ln |A_t - A_\infty|$ against time display a change from one apparent step to two steps as the concentration of the diene rises, so that data can be handled in two ways. Where two steps can be discerned, the second is independent of diene concentration and so corresponds to (2). After correction for the second step,[9] k_{obsd} for the first follows eq 3 and so is identified with (1) (k_a being equivalent to k_1 as before). Alternatively, if k_{obsd} for runs in which there is only one apparent reaction are combined with k_{obsd} for those second steps that can be detected, graphs conforming to eq 5 are obtained. This equation

$$1/k_{obsd} = 1/(k_c[\text{diene}]) + 1/k_d \quad (5)$$

describes a fast initial equilibrium followed by a slower step, viz. (1) followed by (2) here ($k_c \equiv K_1k_2$ and $k_d \equiv k_2$; see Table III). The value of K_1k_2 at 25.0 °C found in this way corresponds reasonably with the rate constant estimated from the NMR runs.

Discussion and Conclusions

Kinetic parameters are given in Table III, while a qualitative idea of relative rates and completeness of reactions is shown in

---

† Univeristy of York.

‡ University of California.

(1) $Na[PdCl_3(OCMe_2)]$ is prepared in situ by mixing anhydrous Na_2PdCl_4 with dry acetone. After 1 h of stirring, there is quantitative precipitation of 1 equiv. of NaCl, which is removed by filtration. The required solutions are obtained by diluting the filtrate with acetone and adding 2% water. In analogous work using pure acetone, NaCl tends to be precipitated, but the kinetics are very similar.

(2) Chatt, J.; Vallarino, L. M.; Venanzi, L. M. *J. Chem. Soc.* **1957**, 3413.
(3) Albelo, G. A.; Rettig, M. F. *J. Organomet. Chem.* **1972**, *42*, 183.
(4) Able, E. W.; Bennett, M. A.; Wilkinson, G. *J. Chem. Soc.* **1959**, 3178.
(5) Zakharova, I. A.; Kukina, G. A.; Kuli-Zada, T. S.; Moiseev, I. I.; Yu Pek, G.; Porai-Koshits, M. A. *Russ. J. Inorg. Chem.* (*Engl. Transl.*) **1966**, *11*, 1364.
(6) The rate is taken as $-d[PtCl_4^{2-}]/dt$, and customary pseudo-first-order conditions are used, so that a plot of $\ln [A_t - A_\infty]$ against times gives k_{obsd} in the usual way.
(7) Espenson, J. H. "Chemical Kinetics and Reaction Mechanisms"; McGraw-Hill: New York, 1981; p 45.
(8) Beck, M. T. "Chemistry of Complex Equilibria"; Van Nostrand-Reinhold: London, 1970; p 91.
(9) Espenson, J. H. "Chemical Kinetics and Reaction Mechanisms"; McGraw-Hill: New York, 1981; p 65.

0020-1669/86/1325-0243$01.50/0